ResearchHub JOURNAL

Transcriptomic Analysis of a Cannabis-Derived Neuroprotective Therapy in a Zebrafish Model of ALS

Ishaan Banwait[1,2], Kelly Boddington[1,3], Eric Soubeyrand[1,3], José A. Casaretto[1,3], Gurkamal Deol[1,4], Farhad Karbassi[5], Akeem Gardner[1*]

Published: October 9, 2025

[1] Canurta Therapeutics, Mississauga, Ontario, Canada
[2] University of Waterloo, Waterloo, Ontario, Canada
[3] University of Guelph, Guelph, Ontario, Canada
[4] Western University, London, Ontario, Canada
[5] CREMCo Labs, Mississauga, Ontario, Canada

*Corresponding author: akeem@canurta.com

ABSTRACT

Amyotrophic lateral sclerosis (ALS) is a progressive neurodegenerative disease characterized by motor neuron loss, and currently has limited therapeutic options. To address the need for more effective therapies, we evaluated CNR-401, a novel cannabis-based multi-component formulation, in a zebrafish model of ALS induced by the neurotoxin β-N-methylamino-L-alanine (BMAA). Zebrafish larvae exposed to BMAA developed characteristic motor dysfunction, validating this model of toxin-induced neurodegeneration. In behavioral assays, CNR-401 significantly rescued BMAA-induced locomotor impairments in a dose-dependent manner, with efficacy observed at concentrations as low as 0.5 μM, exceeding the potency of both Edaravone and cannflavin A, a flavonoid constituent of CNR-401. Transcriptomic profiling revealed distinct patterns of differential gene expression and pathway enrichment associated with disease progression and therapeutic modulation. Our results show that BMAA induces transcriptomic alterations, particularly upregulating genes involved in neuroinflammation and extracellular matrix (ECM) remodeling. Treatment with CNR-401 produced the most extensive differential gene expression changes, with 1,576 significantly altered genes compared to 359 for edaravone and 130 for cannflavin A (Log2FC>1; FDR<0.5). Functional enrichment analyses indicated that CNR-401 reprogrammed pathways related to cytokine signaling, extracellular matrix organization, steroid metabolism, calcium-mediated signaling, and PI3K-Akt signaling, suggesting multi-target neuroprotective mechanisms. In contrast, Edaravone and cannflavin A elicited more limited and distinct transcriptomic changes, with Edaravone primarily affecting metabolic and signaling pathways, and cannflavin A modulating metabolic and steroidogenic pathways. These findings demonstrate that CNR-401 provides functional neuroprotection in a BMAA-induced zebrafish ALS model, which is consistent with the modulation of processes central to ALS pathology, targeting inflammation, excitotoxicity, and metabolic dysregulation. Future studies are needed to validate these results and further define the translational potential of this phytochemical formulation as a therapeutic candidate for ALS.

Keywords
ALS; amyotrophic lateral sclerosis; BMAA; cannabis; cannflavin; transcriptomics; zebrafish

Key Messages

- CNR-401, a multi-component cannabis formulation, rescued BMAA-induced motor deficits in zebrafish with sub-micromolar potency (effective ≥0.5 μM), outperforming edaravone and cannflavin A.
- Transcriptomics showed broad disease-relevant reprogramming with CNR-401 (1,576 DEGs vs 359 with edaravone), down-modulating neuroinflammation and ECM remodeling while engaging steroid, calcium, and PI3K-Akt pathways—consistent with multi-target neuroprotection in ALS.

INTRODUCTION

Amyotrophic lateral sclerosis (ALS) is a rapidly progressive neurodegenerative disorder characterized by the degeneration of motor neurons, leading to muscle weakness, paralysis, and premature death. Current therapies, such as riluzole and edaravone, provide only modest benefits[1], underscoring the urgent need for new therapeutic approaches that address the complex molecular mechanisms underlying ALS pathogenesis.

Animal models have been essential in advancing our understanding of the disease, providing platforms to study disease mechanisms and evaluate therapeutic strategies. Mutations in more than 40 genes have been modeled across species, including rodents, zebrafish, and invertebrates[2]. These models have revealed key pathological processes such as excitotoxicity, oxidative stress, protein misfolding, impaired axonal transport, and neuroinflammation, all of which contribute to motor neuron degeneration. Importantly, animal studies have guided the discovery of small molecules targeting these pathways. Although animal systems continue to provide insights into ALS biology, genetic models of ALS often fail to capture the full spectrum of disease pathology observed in patients. Toxin-based models offer an opportunity to study these influences directly. In particular, β-N-methylamino-L-alanine (BMAA), a cyanobacterial neurotoxin, induces ALS-like phenotypes in animal models, including motor deficits, spinal abnormalities, oxidative stress, and neuromuscular junction disruption[3, 4]. Importantly, human epidemiological data link chronic BMAA exposure to ALS incidence, as evidenced in Chamorro populations of Guam, where high brain BMAA levels correlate with a strikingly elevated ALS-parkinsonism-dementia prevalence[5]. Mechanistically, BMAA drives pathology through excitotoxicity, neuroinflammation, and calcium dysregulation[6, 7].

Zebrafish (Danio rerio) represent a powerful vertebrate model for neurodegenerative research, offering genetic tractability, conserved neurobiology, and suitability for high-throughput screening in preclinical drug discovery. Due to their small size, rapid development, and transparent embryos, which allow real-time visualization of biological processes, zebrafish larvae are increasingly being used in phenotypic assays that evaluate the effects of drug candidates on development, behavior, and disease models[8]. Given zebrafish genetic similarity to humans (70% overall, and 84% of human disease genes with orthologs), a BMAA-induced model of motor

neuron dysfunction in zebrafish can provide a complementary approach to genetic systems, enabling the evaluation of candidate therapeutics.

CNR-401 is a designed phytochemical formulation with unique cannabis bioactive compounds that work synergistically to target neuroinflammatory pathways implicated in ALS, including neuroinflammation, excitotoxicity, oxidative stress, and mitochondrial dysfunction[9-14]. It combines cannabidiol (CBD), cannabinoid acid precursors, select terpenes, and the prenylated flavonoid cannflavin A, which has demonstrated exceptional potency through dual inhibition of mPGES-1 and 5-LOX[15, 16].

Previous transcriptomic studies in ALS models, including rodent genetic knock-ins, zebrafish exposed to neurotoxins, and human iPSC-derived motor neurons, have highlighted pathways related to oxidative stress, mitochondrial dysfunction, and inflammation[17-19]. Similarly, cannabinoid-based interventions, such as CBD or synthetic CB2 agonists, have shown partial neuroprotection in rodent ALS models[20, 21]. However, few studies have combined a multi-component cannabinoid–flavonoid formulation with high-resolution transcriptomic profiling. Zebrafish have conserved cannabinoid receptor systems and neurotransmitters found in mammalian systems[22], making it a useful platform for evaluating cannabinoid-based therapeutics. We first established a BMAA-induced motor neuron dysfunction model in zebrafish larvae, in which Edaravone was able to rescue the ALS-like phenotype. Based on the mechanistic properties of its components, we hypothesize that CNR-401 can counteract BMAA-induced motor neuron degeneration in zebrafish, thereby mitigating ALS-like pathology. This study distinguishes itself by including a multi-component cannabinoid–flavonoid formulation with high-resolution transcriptomic profiling in a zebrafish BMAA model for dissecting disease-relevant molecular pathways. It also directly compares CNR-401's effects with Edaravone, a clinically approved ALS drug, and single-compound controls to detect potential therapeutic targets.

MATERIALS AND METHODS

Zebrafish Husbandry

Wild-type zebrafish (*Danio rerio*, AB strain) were maintained at 28.5 °C under a 14-hour light and 10-hour dark cycle. Maintenance and husbandry of the animals used in this study were conducted in accordance with the guidelines of the Canadian Council on Animal Care (CCAC) and mated to produce embryos for experimentation. Larvae were incubated at 28.5°C for 5 days, fed brine shrimp, and screened for overall health and development before use.

Solvent Toxicity Assessment

Solubilizers were necessary to make cannabinoids and terpenes in the test formulations miscible in water, as these compounds are inherently not water-soluble, creating challenges for aquatic organism testing. Two cyclodextrin solubilizers, which are utilized in several commercially available drugs, were evaluated: hydroxypropyl-β-cyclodextrin (HPC) and hydroxyethyl-β-cyclodextrin (HEC). For each cyclodextrin, toxicity assays were completed at 6 days post-treatment and performed at concentrations of 0, 0.5, 1, 5, 10, and 20 mM prepared in water. HPC demonstrated significant toxicity at 5 mM concentration, resulting in 75% larval mortality

with observable toxicity in surviving larvae, including cardiac edema, abnormal heart rate, and complete mortality observed at 10 mM and 20 mM. In contrast, HEC showed no toxicity up to 20 mM, with all larvae surviving and displaying no morphological changes or significant decrease in movement. Based on these results, all subsequent efficacy assessment experiments were performed using 10 mM HEC as the final concentration.

Product Toxicity Assessment

Toxicity assessments were performed on CNR-401 and cannflavin A (CNR-402a) at final concentrations of 0, 0.5, 1, 2, 5, and 10 µM. CNR-401 concentrations were expressed in terms of CBD-equivalent, as it is the principal and most abundant active component of the complex botanical mixture. All toxicity assays were completed at 6 days post-treatment with 10 mM HEC in all conditions. Diluted solutions were prepared in 10 mM HEC 5-10 minutes before addition to multi-well plates.

Product Efficacy Assessment and Phenotypic Analysis

At 8 hours post-fertilization, zebrafish embryos were distributed into 48-well plates (1 larva per well) and exposed to BMAA at optimized concentrations to induce ALS-like neurodegeneration. Test compounds (CNR-401 and cannflavin A) were administered at their respective no-observed-adverse-effect level (NOAEL) final concentration with 10 mM HEC. Each experimental plate contained non-treated controls (10 mM HEC as solubilizer only), BMAA-treated controls, and BMAA + compound-treated wells (8 wells per condition). Edaravone, the currently available ALS medication, was included as a positive control. Eight wells, each containing one larva, were used for each of the treated and non-treated groups mentioned and repeated in at least six independent experiments. Plates were incubated at 28°C throughout the experimental period. Behavioral assessments were conducted using the DanioVision™ automated behavioral tracking system (Noldus Information Technology, Wageningen, The Netherlands) equipped with a GigE camera. At 6 days post-fertilization, zebrafish larvae were exposed to white light (15-16 $\mu M \cdot s^{-1} \cdot m^{-2}$) for 1 minute, followed by tracking for 20 minutes under light conditions. Locomotion patterns were recorded and analyzed using EthoVision XT17 software (Noldus Information Technology) to generate comprehensive behavioral profiles. Following behavioral recording, larvae were visually examined to assess phenotypic responses and remove any dead, necrotic, or morphologically affected specimens from the analysis. Visual assessments included evaluation of cardiac edema, abnormal heart rate, body deformation, and overall morphological integrity. Only larvae displaying normal morphology and survival were included in the final behavioral analysis to ensure data quality and experimental validity. Distance moved (mm) served as the primary behavioral endpoint, with BMAA treatment expected to significantly reduce locomotion compared to untreated controls. Effective neuroprotective compounds were anticipated to demonstrate rescue effects by restoring locomotor activity toward control levels.

Experimental Conditions and Replication

To investigate transcriptomic responses to neuroprotective therapies in a zebrafish model of ALS, we designed a multi-condition experiment utilizing six biological replicates per group. Zebrafish embryos were randomly assigned to one of five experimental conditions:

- Control: Untreated zebrafish embryos, serving as the baseline reference (HEC only).

- BMAA: Embryos exposed to β-N-methylamino-L-alanine to induce neurodegenerative phenotypes characteristic of ALS.
- CNR-401: BMAA-exposed embryos subsequently treated with drug candidate CNR-401.
- Edaravone: BMAA-exposed embryos subsequently treated with Edaravone, a clinically approved ALS therapy.
- Cannflavin A: BMAA-exposed embryos subsequently treated with pure cannflavin A.

Sample Preparation and RNA Sequencing

Non-control zebrafish embryos were exposed to BMAA to induce neurodegeneration, with additional groups receiving candidate neuroprotective agents, including Edaravone and CNR-401. All samples (non-treated and treated) were prepared in 10 mM HEC. Samples were incubated in 48-well plates in the same manner as the efficacy assay plates. After collection of the larvae and transfer into 2 mL tubes, the samples were washed three times with E3 water (5 mM NaCl, 0.17 mM KCl, 0.33 mM $CaCl_2 \cdot 2H_2O$, 0.33 mM $MgSO_4 \cdot 7H_2O$, pH 7.2). The remaining E3 water was then removed as thoroughly as possible. Samples were flash-frozen in liquid nitrogen and immediately stored at -80 °C. RNA was extracted using the Qiagen RNeasy kit, and libraries were prepared with the Illumina TruSeq Stranded RNA kit. Sequencing was performed on an Illumina NovaSeq 6000 platform using v1.5 2x150 bp chemistry, and yielding an average of 36.3 million read pairs per sample.

Data Processing and Visualization

Raw reads were trimmed with Cutadapt[23] and mapped to the *Danio rerio* reference genome assembly GRCz11 using STAR 2.7.11b[24, 25]. FastQC[26] was used to analyze the quality of the reads before and after trimming. Gene-level counts were subsequently imported into DESeq2 (v.1.44.0)[27] for normalization and pairwise differential expression analysis (with ~batch + condition design). An adjusted p-value (padj, q) false discovery rate (FDR) of 0.05 (Benjamini and Hochberg) was used as the cutoff value for downstream analysis. In this study, a next-generation differential expressed gene (DEGs) Pipeline Assistant developed by Canurta Therapeutics was employed[28]. This analysis platform is comparable to existing tools, but was specifically designed for high-throughput, reproducible, and pathway-oriented interpretation of RNA-seq data. The pipeline integrates advanced normalization, automated gene–pathway curation, and streamlined reproducibility, accelerating the identification of candidate therapeutic targets relevant to ALS. The downstream analysis included: automated metadata construction and quality control (boxplots, correlation heatmap, PCA), differential expression filtering with log2 fold change > 1 and adjusted p-value < 0.05, visualization (MA plots, volcano plots, heatmaps), ortholog mapping to human genes, and GO and KEGG functional enrichment analysis with adjusted p-value < 0.05. A summary of the parameters used is presented in the Supplementary Material.

RESULTS

Product Toxicity Assessment

Both CNR-401 and cannflavin A demonstrated no toxicity up to 2 µM concentration (Supplementary Material: Product Toxicity Assays). Acute toxicity assays were conducted to determine the median lethal concentration (LC_{50}), which is the concentration of the product estimated to be lethal to 50% of the test organisms within the test duration. CNR-401 showed

62.5% larval survival at 5 µM and complete mortality at 10 µM, yielding an LC_{50} of 4.82 µM. Cannflavin A exhibited 37.5% survival at 5 µM and complete mortality at 10 µM, with an LC_{50} of 4.69 µM. Teratotoxicity assessments closely followed acute toxicity trends for both compounds. Given that both products were safe up to a final concentration of 2 µM, the assays were repeated in three independent experiments in order to explore the toxicity between 2 and 5 µM and to identify the NOAEL, which represents the maximum safe concentration.

Product Efficacy Assessment

BMAA treatment significantly reduced locomotion in zebrafish larvae ($p < 0.0001$), confirming the validity of the neurodegeneration model. Edaravone, a current ALS medication, demonstrated significant rescue effects ($p = 0.0002$) on BMAA-treated larvae mobility. Both CNR-401 and cannflavin A showed significant rescue effects with p-values of $p < 0.0001$ and $p = 0.0054$, respectively (Figure 1A). All treatments were administered at a 2 µM concentration. CNR-401 displayed dose-dependent efficacy with the lowest effective dose of 0.5 µM in the BMAA-induced neurotoxicity model (Figure 1B), exhibiting an estimated EC_{50} of 0.0012 µM. Cannflavin A required a higher concentration, showing efficacy beginning at 1 µM with an estimated EC_{50} of 0.004 µM (Figure 1C). This difference indicates superior potency for CNR-401 at lower concentrations.

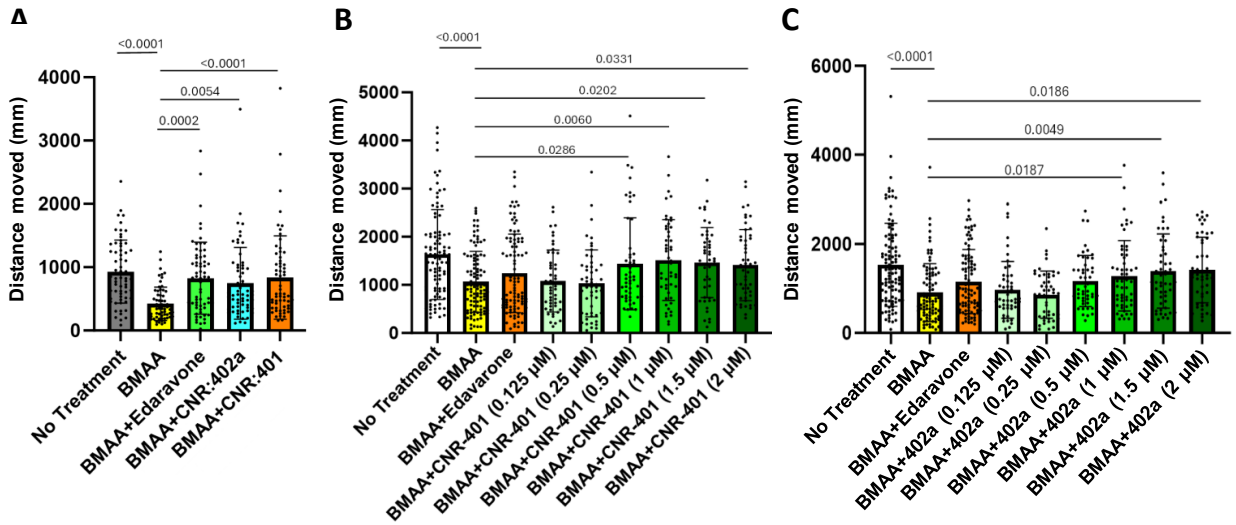

Figure 1. Effect of CNR formulations in restoring motility in a BMAA-induced zebrafish model of motor neuron dysfunction. **(A)** Treatments with CNR-401 and cannflavin A (CNR-402a) dosed at 2 µM. Bars represent mean ± SD of six independent experiments for the 'BMAA + CNR401' condition, and nine for all other conditions, each with eight larvae (biological replicates). **(B)** Dose response of CNR-401 and **(C)** dose response of cannflavin A (402a) compared to Edaravone at 2 µM, in the same BMAA-induced zebrafish model. Bars in (B) and (C) represent mean ± SD. Dead larvae were excluded from the analysis. In all three graphs, statistical values indicate significant differences from BMAA treatment by 2-way ANOVA with post-hoc Dunnett's multiple comparison test.

Transcriptomic Data Quality

Quality control assessment through boxplot visualization (Supplementary Material: Plots) confirmed excellent data consistency across the biological replicates within each condition group. The normalized gene expression counts displayed uniform distribution patterns with median expression levels aligned across all six replicates for each condition, indicating successful normalization and comparable library sizes. The characteristic compression of interquartile ranges near zero reflects the expected transcriptomic landscape where the majority of genes exhibit low to moderate expression levels.

Consistent outlier patterns extending to approximately 500,000 normalized counts were observed across all samples, representing highly expressed genes such as housekeeping proteins that were reproducibly detected. This uniform distribution profile, combined with the absence of sample-specific technical artifacts or batch effects, demonstrates robust experimental reproducibility and validates the dataset's suitability for downstream differential expression analysis. The boxplot patterns align with established quality standards for normalized RNA-seq data, confirming that technical variation has been effectively minimized while preserving genuine biological signals. The sample correlation analysis (Figure 2) demonstrated high reproducibility within experimental groups, with control samples showing strong internal correlations ($r > 0.90$).

Treatment groups exhibited distinct expression profiles compared to controls, as evidenced by the hierarchical clustering pattern that segregated samples by treatment condition, suggesting that the observed gene expression changes are treatment-specific rather than due to technical variability. A principal component analysis (PCA; Supplementary Material: Plots) revealed substantial variability in gene expression profiles across experimental conditions. Control samples showed considerable dispersion across the PCA space, with replicates distributed from the bottom region (PC1 >= 150, PC2 ≈−150) to the upper right quadrant (PC1 ≈150, PC2 ≈50), indicating significant baseline heterogeneity in untreated samples. BMAA treatment and therapeutic interventions (CNR401, Edaravone, and cannflavin A) showed similarly dispersed patterns across both components, which together explain 38.04% of the total variance. The observed dispersion could be reflecting effects from different batches or plates. This variability in RNA-seq data aligns with established norms[29].

Differentially Expressed Genes

Differential gene expression analysis between BMAA-affected and treated conditions revealed distinct responses across the three test compounds (Figures 5-6). CNR-401 treatment resulted in 1,576 significantly differentially expressed genes (DEGs), while Edaravone treatment showed 359 DEGs, and cannflavin A treatment showed 130 DEGs (Table 1). These findings are represented in MA plots illustrating the transcriptomic changes of BMAA exposure and subsequent treatments in zebrafish (Figure 3). Comparison of BMAA-affected versus control embryos reveals widespread differential gene expression, with numerous genes significantly dysregulated, reflecting the broad molecular disruption induced by BMAA. Treatment with Edaravone led to a moderate degree of gene expression changes relative to BMAA alone, showing a limited but detectable transcriptomic response. In contrast, CNR-401 treatment produced a greater number

of DEGs, indicating more extensive reprogramming of BMAA-induced molecular alterations, while cannflavin A induced the fewest transcriptomic changes.

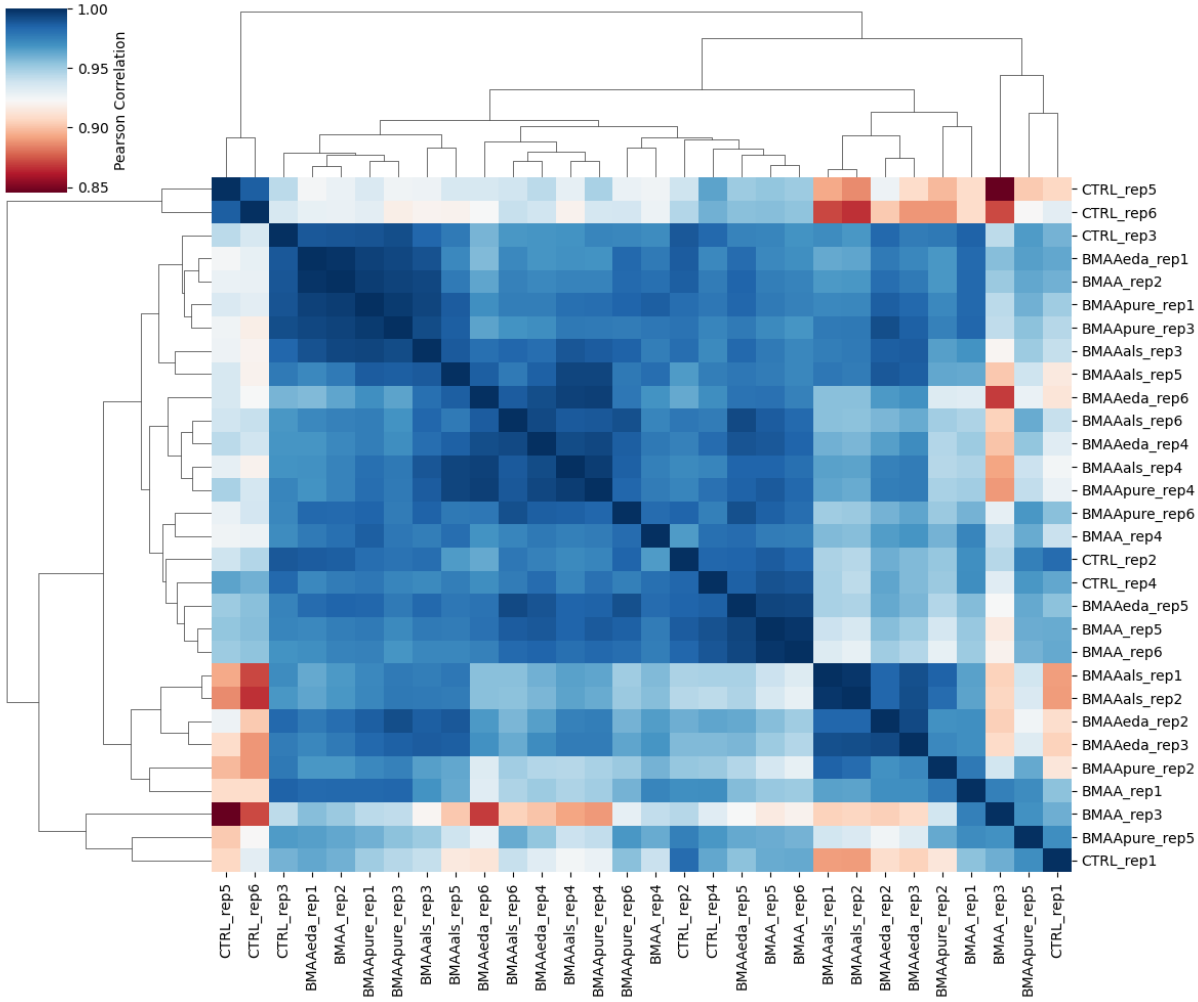

Figure 2. Heatmap showing pairwise Pearson correlations of gene expression between all samples, clustered hierarchically (CTRL, No BMAA control; BMAA, BMAA-treated; BMAAals, BMAA + CNR401; BMAApure, BMAA + cannflavin A; and BMAAeda, BMAA + Edaravone). A darker blue square indicates a stronger positive correlation, as seen in the squares along the diagonal showing a perfect self-correlation ($r = 1.0$).

Figure 4 presents volcano plots highlighting both the magnitude of gene expression changes (log2 fold change) and their statistical significance (–log10 adjusted p-value) across the same four comparisons. Notably, there were more downregulated genes in BMAA exposure compared to control, and with treatments with Edaravone and CNR-401, while cannflavin A showed the fewest significant gene expression changes, with limited clusters of up- and downregulated genes.

Overall, these plots demonstrate that while all treatments modulate BMAA-driven transcriptomic dysregulation to varying degrees, CNR-401 exhibits the most extensive and statistically significant impact, suggesting a role as a multi-target therapeutic candidate. Venn diagrams of upregulated and downregulated zebrafish DEGs illustrate how many common and unique DEGs are present in the three treatments versus BMAA (Figures 5A, 5B). CNR-401 exhibited the largest number of up- and downregulated DEGs, suggesting broad transcriptomic modulation and potential multi-target effects compared to single-compound treatments.

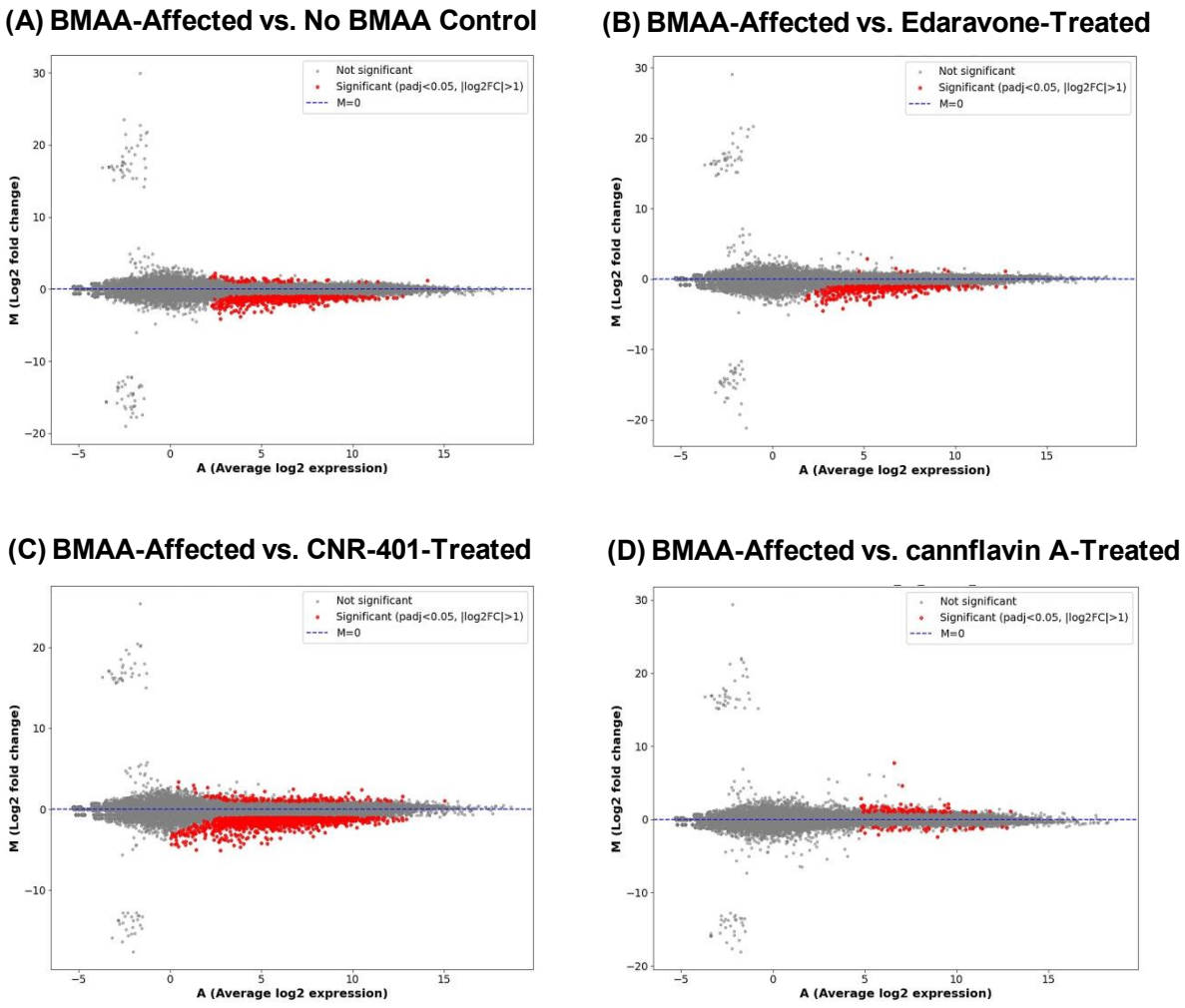

Figure 3. MA plots showing differential gene expression analysis between BMAA-affected and treated conditions. **(A)** BMAA-affected vs. control; **(B)** BMAA-affected vs. Edaravone-treated; **(C)** BMAA-affected vs. CNR-401-treated; **(D)** BMAA-affected vs. cannflavin A-treated. In the graphs, each point represents a gene plotted by average log2 expression (A, x-axis) versus log2 fold change (M, y-axis). Red points indicate significantly differentially expressed genes.

DOI: 10.55277/rhj.tv4dbb3e.5

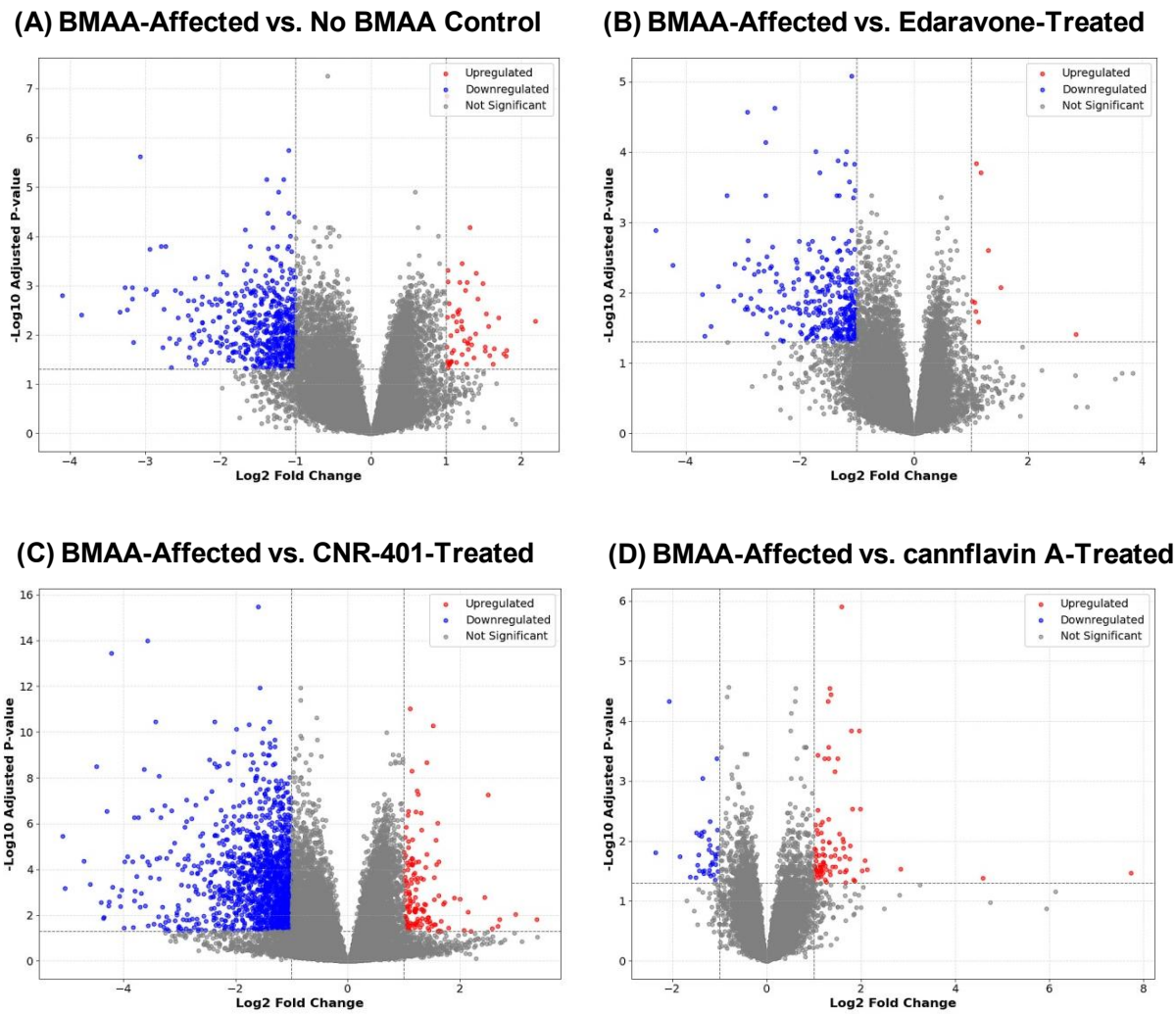

Figure 4. Volcano plots of differential gene expression, showing statistical significance versus biological significance. **(A)** BMAA-affected vs. control; **(B)** BMAA-affected vs. Edaravone-treated; **(C)** BMAA-affected vs. CNR-401-treated; **(D)** BMAA-affected vs. cannflavin A-treated. In the graphs, each point represents a gene, with log2 fold change on the x-axis and –log10 adjusted p-value on the y-axis. Significantly downregulated genes are shown in blue, and significantly upregulated genes are shown in red.

Mapping the significantly DEGs from the BMAA-affected versus CNR-401-treated comparison to their human orthologs revealed that the majority were downregulated. The total numbers can be appreciated in the Venn diagrams, which illustrate the distribution of shared and unique human ortholog genes across treatment conditions (Figures 5C, 5D). Of the top genes (Table 2), the first 19 belong to the *UGT* gene family, which are mapped from the same underlying zebrafish gene transcript, explaining the identical or nearly identical expression values. This ortholog mapping indicates downregulation of the *UGT* family rather than independent measurements. In the BMAA vs. control comparison, this family of orthologs showed only

approximately a -0.5 log2 fold change (Supplementary Material: Data), demonstrating the significant impact of CNR-401 on these genes.

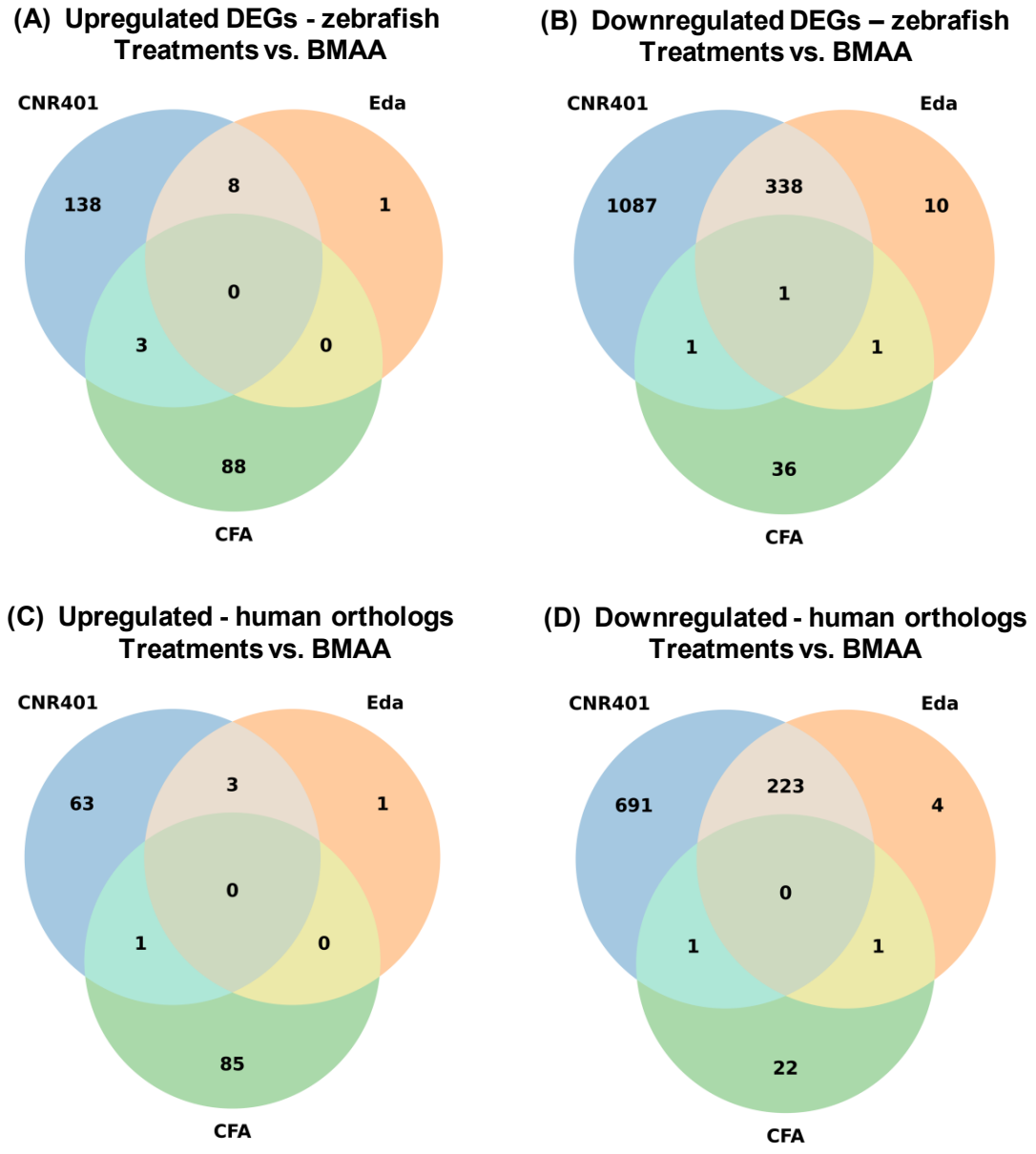

Figure 5. Venn diagrams of common and unique differentially expressed genes (DEGs) following treatments compared to BMAA exposure. **(A)** Upregulated and **(B)** downregulated DEGs identified from RNA-seq analysis of zebrafish larvae treated with CNR-401, Edaravone (Eda), or cannflavin A (CFA) relative to BMAA-exposed samples. **(C)** and **(D)** display the number of corresponding human orthologs found for the zebrafish DEGs shown in (A) and (B), respectively, in the same treatment comparisons.

Table 1. Summary of pairwise comparisons of interest.

Comparison	Total Genes	Significant Genes	Upregulated	Downregulated
BMAA vs Control	28788	624	57	567
BMAA vs BMAA + CNR401	28788	1576	149	1427
BMAA vs BMAA + Edaravone	28788	359	9	350
BMAA vs BMAA + Cannflavin A	28788	130	91	39

Table 2. Top human orthologs (sorted by L2FC) differentially expressed when BMAA-affected samples were treated with CNR401.

Ortholog Name	Description	Absolute L2FC	Expression	Adjusted P-Value
UGT1A (8) UGT2A (3) UGT2B (7) UGT3A (1)	19 members of UDP glucuronosyltransferase genes, families 1, 2, and 3	4.077694	Downregulated	0.001473
URGCP	upregulator of cell proliferation	3.702947	Downregulated	0.004319
DAO	D-amino acid oxidase	3.68739	Downregulated	0.001132
SDR42E2	short chain dehydrogenase/reductase family 42E; member 2	3.663107	Downregulated	2.6795e-05
GBP6	guanylate binding protein family member 6	3.558249	Downregulated	0.028347
MXRA5	matrix remodeling associated 5	3.424166	Downregulated	3.6191e-11
NOTCH4	notch receptor 4	3.15797	Downregulated	1.6582e-05
B3GALT9	beta-1;3-galactosyltransferase 9	3.018835	Downregulated	0.005205
HLA-DQA1 HLA-DQA2	major histocompatibility complex; class II; DQ alpha 1 and 2	3.016801	Downregulated	0.034057
UNG	uracil DNA glycosylase	2.996153	Upregulated	0.009045
COL6A3	collagen type VI alpha 3 chain	2.950076	Downregulated	9.9005e-05

Functional Enrichments

Enrichment analysis of gene ontology (GO) biological process revealed that, in the BMAA versus BMAA+CNR401 comparison (Figure 6B), the most significantly enriched terms included extracellular matrix organization, external encapsulating structure organization, cellular response to cytokine stimulus, extracellular structure organization, cytokine-mediated signaling pathway, steroid metabolic process, estrogen metabolic process, calcium-mediated signaling, inflammatory response, and regulation of angiogenesis. For the BMAA versus control

comparison (Figure 6A), enriched GO biological processes included cellular response to cytokine stimulus, cellular response to growth hormone stimulus, growth hormone receptor signaling pathway, cytokine-mediated signaling pathway, extracellular matrix organization, sulfation, ethanol catabolic process, positive regulation of receptor signaling pathway via STAT, ethanol metabolic process, and external encapsulating structure organization.

To define the pathways that were most affected, a Kyoto Encyclopedia of Genes and Genomes (KEGG) enrichment analysis showed that, in the BMAA versus BMAA+CNR401 comparison (Figure 6D), the top enriched pathways were cytokine-cytokine receptor interaction, steroid hormone biosynthesis, ascorbate and aldarate metabolism, porphyrin and chlorophyll metabolism, pentose and glucuronate interconversions, bile secretion, PI3K-Akt signaling pathway, metabolism of xenobiotics by cytochrome P450, ovarian steroidogenesis, and retinol metabolism. In the BMAA versus control comparison (Figure 6C), enriched KEGG pathways included the JAK-STAT signaling pathway, PI3K-Akt signaling pathway, pathways in cancer, cytokine-cytokine receptor interaction, ovarian steroidogenesis, ECM-receptor interaction, Th17 cell differentiation, choline metabolism in cancer, human papillomavirus infection, and small cell lung cancer.

DISCUSSION

CNR-401 Induces Broad Transcriptomic Changes in BMAA-Exposed Zebrafish

Transcriptomic analysis demonstrated that CNR-401 treatment produced more changes in gene expression than either Edaravone or cannflavin A in the BMAA zebrafish model of ALS. In the BMAA + CNR-401 group, 1,576 genes were significantly differentially expressed, compared to 359 with Edaravone and only 130 with cannflavin A. Most genes (1,427) were downregulated, while 149 were upregulated, indicating that CNR-401 primarily suppresses pathological expression changes induced by BMAA, and suggests that CNR-401 mitigates BMAA-driven molecular variations across multiple pathways, consistent with a multi-target neuroprotective mechanism. Importantly, these transcriptomic changes were accompanied by improved functional mobility observed in vivo, confirming that widespread gene modulation was not detrimental but rather aligned with a therapeutic benefit.

Among the most notable differentially expressed genes was one coding for a UDP-glucuronosyltransferase (UGT) family, which was strongly downregulated. UGT enzymes normally detoxify xenobiotics through glucuronidation[30]. Its suppression suggests that CNR-401 either reduces BMAA toxicity by alternative mechanisms or decreases reliance on endogenous detoxification pathways. Additionally, lower UGT expression may preserve neuroprotective steroid levels, as UGTs also conjugate and eliminate steroids.

Other ALS-relevant genes were similarly modulated. URGCP, a driver of cell proliferation via Wnt/β-catenin signaling[31], was reduced. Since glial proliferation contributes to neuroinflammation and scarring[32], and URGCP/Wnt signaling has been shown to dampen microglial activation and neuroinflammation[33], this downregulation suggests that CNR-401 may be reducing pathological gliosis. DAO (D-amino acid oxidase) was also downregulated, aligning with reduced excitotoxicity. DAO inactivation in astrocytes protects against D-serine–mediated

motor neuron injury[34]. While DAO loss-of-function can have complex, context-dependent effects[35], CNR-401's anti-excitotoxic and antioxidant properties could mitigate potential risks, as evidenced by preserved motor function in vivo. CNR-401 also suppressed MXRA5, a regulator of extracellular matrix (ECM) remodeling that promotes MMP-9 (matrix metalloproteinase-9, an enzyme that breaks down ECM proteins) activation and blood–spinal cord barrier disruption[36]. This likely reflects modulation of the TGF-β1 pathway, which regulates ECM homeostasis[37]. Gene ontology enrichment confirmed ECM-related processes among the top pathways altered by CNR-401, suggesting that they may contribute to an improved structural integrity of neural tissues.

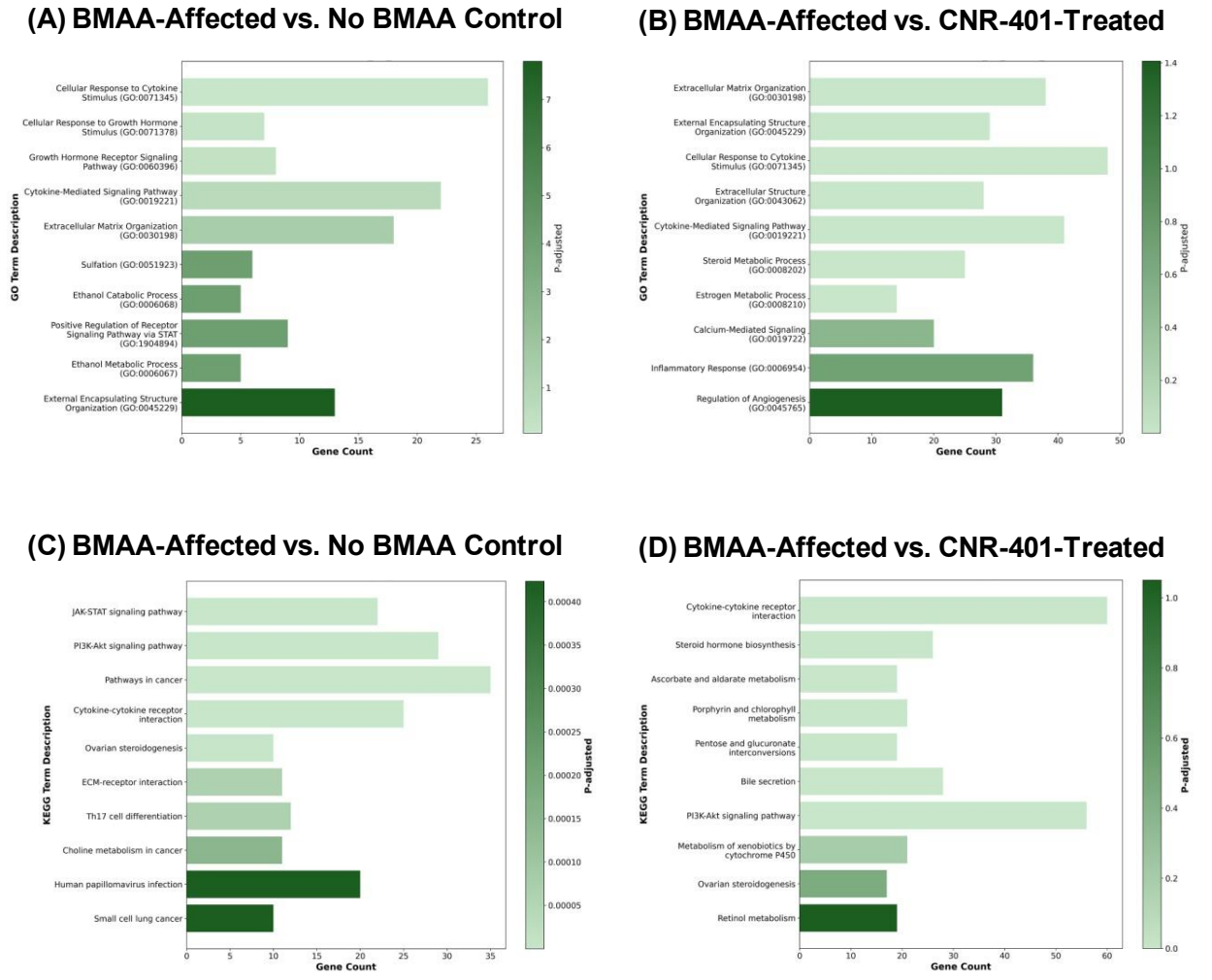

Figure 6. (A, B) GO biological process (BP) enrichment analysis of differentially expressed genes between pairwise comparisons of interest is indicated. **(C, D)** KEGG pathway enrichment analysis of differentially expressed genes in each experimental comparison. **(A, C)** BMAA-affected vs. control; **(B, D)** BMAA-affected vs. CNR-401-treated. In all graphs, bar length represents the number of genes associated with each enriched GO term or pathway, and color intensity reflects the adjusted p-value for enrichment significance.

Neuroimmune activation markers were also downregulated. Expression of the ortholog of two MHC class II immune genes, HLA-DQA1 and HLA-DQA2, was reduced. Normally absent in the CNS, these genes are upregulated in microglia during inflammation[38-40]. Its suppression is consistent with CNR-401's anti-inflammatory profile, limiting CD4+ T cell activation and microglial reactivity. In contrast, UNG (uracil-DNA glycosylase) was one of the few genes upregulated. UNG is central to base-excision repair, correcting oxidative DNA lesions[41]. Its increased expression suggests a response to enhance DNA repair capacity, which could protect motor neurons from cumulative damage induced by BMAA toxicity[42, 43].

Enriched Biological Processes and Pathways in CNR-401 Treatment

Gene Ontology (GO) enrichment analysis highlights extracellular matrix (ECM) organization and inflammatory response as two primary biological processes altered by BMAA exposure and modulated by CNR-401. ECM breakdown is a well-established pathological feature in neurodegenerative diseases. For instance, in multiple sclerosis, damaged ECM components amplify inflammation[44], and in ALS, ECM degradation destabilizes neural tissue, activating microglia and creating a self-perpetuating cycle of chronic inflammation and further ECM damage[45]. Our findings demonstrate enrichment of ECM-related terms – "extracellular matrix organization," "external encapsulating structure organization," and "extracellular structure organization" – associating CNR-401 activity with stabilization of ECM integrity. At the same time, inflammatory response pathways such as "inflammatory response," "cytokine-mediated signaling pathway," and "cellular response to cytokine stimulus" appeared as major enriched processes. Neuroinflammation is now recognized as a primary driver of ALS pathology rather than a secondary consequence. Studies with chimeric mice demonstrate that wild-type neurons develop ALS phenotypes when surrounded by glia expressing mutant proteins, confirming the non-cell autonomous nature of motor neuron injury[46]. ALS neuroinflammation involves peripheral lymphocyte infiltration, activation of microglia and astrocytes, and complement cascade engagement, all contributing to neurotoxicity through pro-inflammatory cytokines and oxidative stress[47]. Thus, modulation of ECM and inflammatory processes by CNR-401 treatment suggests a dual mechanism that targets two contributors to motor neuron degeneration.

Beyond these important processes, other enriched terms indicate that CNR-401 can affect calcium signaling and steroid metabolism. Motor neurons are intrinsically vulnerable to calcium dysregulation, with high expression of calcium-permeable AMPA receptors and poor buffering capacity[48]. Excitotoxic cascades drive a "toxic shift" in the ER-mitochondrial calcium cycle, culminating in mitochondrial and cytosolic calcium accumulation[49, 50]. The enrichment of calcium-mediated signaling processes after CNR-401 treatment implies restoration of calcium homeostasis, reducing excitotoxic stress. Steroid metabolic pathways were also enriched, with a notable focus on estrogen metabolism. This correlates with downregulation of UDP-glucuronosyltransferase (UGT) enzymes, which normally conjugate and inactivate neurosteroids. By suppressing UGTs, CNR-401 may prolong the activity of neuroprotective steroids such as progesterone metabolites and 17β-estradiol, which regulate calcium homeostasis, inflammation, and apoptosis[51-57]. This suggests a therapeutic effect that could enhance endogenous neuroprotective signaling without requiring hormone supplementation. Nonetheless,

downregulation of UGT genes and the potential effect on neurosteroid levels remain to be confirmed.

The above-mentioned findings are supported by a KEGG pathway enrichment analysis. "Cytokine-cytokine receptor interaction" emerged as the top pathway, underscoring CNR-401's effects on immunomodulation. Enrichment of "steroid hormone biosynthesis" and "ovarian steroidogenesis" pathways validated the GO-based interpretation, situating UGT downregulation within the larger context of steroid network modulation. Additional enriched pathways, including "ascorbate and aldarate metabolism" and "retinol metabolism," highlight antioxidant contributions from vitamins C and A[58–61]. Finally, detoxification pathways ("pentose and glucuronate interconversions," "metabolism of xenobiotics by cytochrome P450") indicate systemic effects on Phase I/II metabolism, where downregulation of UGT enzymes reduces glucuronidation burden[62-65].
KEGG pathway analysis revealed additional mechanisms beyond GO enrichment, most notably the enrichment of the PI3K-Akt signaling pathway. This pathway is a central regulator of neuronal survival and has been widely implicated in neuroprotective processes across neurodegenerative diseases[66]. PI3K-Akt signaling promotes neuronal resilience by stimulating proliferation, inhibiting apoptosis, and modulating stress responses, including oxidative and inflammatory signaling[67]. Studies in SOD1-G93A mouse models of ALS have demonstrated that treatments enhancing PI3K-Akt activity slow disease progression, improve motor performance, and reduce pathological alterations[68]. Accordingly, enrichment of this pathway suggests that CNR-401's neuroprotective activity may be in part due to activating survival cascades that mitigate BMAA-induced oxidative stress, inflammation, and cell death. Comparison with BMAA versus control enrichment demonstrated that BMAA exposure activates pathological pathways such as JAK-STAT, PI3K-Akt, cytokine-receptor interaction, and ECM-receptor interaction, consistent with inflammatory and degenerative responses. In contrast, CNR-401 enrichment patterns point to counteracting these processes, implying a therapeutic specificity. Together, KEGG and GO enrichment analyses indicate that CNR-401 may contribute to the modulation of key pathogenic processes – cytokine signaling, steroid metabolism, antioxidant defense, detoxification, and cell survival – supporting its potential to slow ALS progression through coordinated multi-target neuroprotection.

Comparative Transcriptomic Signatures of CNR-401, Edaravone, and Cannflavin A
Comparing CNR-401 with edaravone and cannflavin A highlights distinct mechanistic profiles that could account for their differing therapeutic effects. Edaravone, an FDA-approved ALS therapy, acts primarily as a free radical scavenger, mitigating oxidative stress and slowing motor neuron deterioration[1, 69]. Its neuroprotection derives from direct neutralization of reactive oxygen species, functioning more as a chemical antioxidant than a transcriptional regulator. In our zebrafish ALS model, Edaravone exposure after BMAA led to 359 differentially expressed genes (DEGs), mostly downregulated. However, enrichment analysis revealed no oxidative stress-related pathways, instead implicating metabolic functions such as steroid biosynthesis, lipid metabolism, and alcohol metabolism, as well as signaling networks like PI3K-Akt, VEGF, and JAK-STAT (Supplementary Material: Results).

Cannflavin A demonstrated a contrasting signature, yielding 130 DEGs (91 upregulated, 39 downregulated). Enrichment analysis unexpectedly showed no significant activation of inflammatory pathways despite its reported anti-inflammatory activity[15, 16]. Instead, modulation was concentrated in metabolic, antioxidant, and steroidogenic functions (Supplementary Material: Results). This discrepancy may be due to in vivo bioavailability, as tissue concentrations at 2 μM could remain insufficient to inhibit its canonical enzyme targets (mPGES-1 and 5-LOX)[15, 70]. Nonetheless, cannflavin A improved locomotor function in BMAA-exposed zebrafish, implying neuroprotective effects even without affecting modulation of inflammatory pathways. However, it did not reproduce CNR-401's wide transcriptional effects, such as UGT downregulation, DNA repair enzyme upregulation, or PI3K-Akt activation.

On the other hand, CNR-401 displayed a more integrated transcriptomic signature, producing modulation across oxidative stress, excitotoxicity, neuroinflammation, calcium regulation, survival signaling, and DNA repair. CNR-401 triggered strong anti-inflammatory responses, including significant downregulation of cytokine signaling and MHC-II genes (HLA-DQA1/DQA2). This contrasted with cannflavin A, which, at the same concentration, failed to enrich these pathways. The enhanced extent of CNR-401's anti-inflammatory signature is likely due to its complex botanical composition, where additive or synergistic interactions among its active constituents contribute to more pronounced effects[14].

In summary, our study suggests that CNR-401 achieves neuroprotection in the zebrafish ALS model through a multi-pathway molecular response. Transcriptomic profiling revealed that CNR-401 could be acting through interrelated mechanisms central to ALS pathology, such as suppression of neuroinflammation and stabilization of the extracellular matrix, modulation of detoxification pathways through UGT downregulation, neurosteroid biosynthesis, mitigation of excitotoxicity, reinforcement of antioxidant defenses, regulation of calcium overload, activation of DNA repair processes, and stimulation of neuronal survival via PI3K-Akt signaling. Collectively, these transcriptomic changes represent a potential therapeutic reorientation toward protection, reducing toxic stress and adverse immune activity, preserving structural integrity, and supporting repair and survival mechanisms. Importantly, these molecular changes translated into significant functional rescue of locomotor deficits in BMAA-exposed zebrafish, indicating that CNR-401 confers neuroprotection. Whereas Edaravone exerted scattered, limited effects and cannflavin A produced selective but narrow modulation, CNR-401 caused combined changes that integrate anti-inflammatory, metabolic, and survival-promoting mechanisms.

As with any transcriptomic study, there exists the need to validate changes in single transcripts or protein levels to verify their biological relevance. The findings of this study also highlight the complexity of transcriptomic profiling in evaluating ALS therapeutics. The difference in the extent of transcriptomic changes between CNR-401 and Edaravone could suggest a more comprehensive therapeutic mechanism. For instance, the downregulation of genes like DAO illustrates that not all changes are inherently beneficial, underscoring the need to pair transcriptomic data with functional outcomes. In effect, Edaravone achieved comparable recovery of BMAA-induced motor deficits with a narrower molecular footprint than CNR-401, implying that modulation of specific pathways may achieve significant outcomes without large

transcriptomic changes. This raises the possibility that CNR-401's broader reprogramming could prove advantageous under more complex or chronic ALS contexts not represented in the toxin-induced model.

Considering the limitations of the approach used in the present work, future studies should extend testing of other genetic ALS models (e.g., mammalian) to validate whether the transcriptomic shifts observed here align with biochemical markers of disease modification and functional improvement. The BMAA-induced zebrafish model provides insight into molecular and phenotypic responses to CNR-401 and neuroprotective mechanisms, but is limited in its ability to fully recapitulate the chronic and multifactorial nature of the human disease. Its translational relevance remains to be confirmed in more complex systems that better approximate mammalian neurobiology. Moreover, as the model captures only short-term effects of treatment, the long-term efficacy and durability of CNR-401's neuroprotective actions in chronic neurodegeneration remain to be determined. Overall, the combination of expanded molecular reprogramming and the observed phenotypic benefit positions CNR-401 as a promising multi-target ALS therapeutic, warranting deeper mechanistic investigation and preclinical validation.

REFERENCES

1. Xu X, Shen D, Gao Y, Zhou Q, Ni Y, Meng H, Shi H, Le W, Chen S, Chen S (2021). A perspective on therapies for amyotrophic lateral sclerosis: can disease progression be curbed? Transl Neurodegener. 10(1): 29. doi: 10.1186/s40035-021-00250-5.
2. Lescouzères L, Patten SA (2024). Promising animal models for amyotrophic lateral sclerosis drug discovery: a comprehensive update. Expert Opin Drug Discov 19(10): 1213–1233. https://doi.org/10.1080/17460441.2024.2387791
3. Oliveira NAS, Pinho BR, Oliveira JMA (2023). Swimming against ALS: How to model disease in zebrafish for pathophysiological and behavioral studies. Neurosci Biobehav Rev 148: 105138. https://doi.org/10.1016/j.neubiorev.2023.105138
4. Newell ME, Adhikari S, Halden RU. (2022) Systematic and state-of-the-science review of the role of environmental factors in amyotrophic lateral sclerosis (ALS) or Lou Gehrig's disease. Sci Total Environ. 817: 152504. doi: 10.1016/j.scitotenv.2021.152504.
5. Cox PA, Banack SA, Murch SJ (2003). Biomagnification of cyanobacterial neurotoxins and neurodegenerative disease among the Chamorro people of Guam. Proc Nat Acad Sci. USA 100(23): 13380-13383. https://doi.org/10.1073/pnas.2235808100
6. Lopicic S, Svirčev Z, Malešević TP, Kopitović A, Ivanovska A, Meriluoto J (2022). Environmental neurotoxin β-N-methylamino-L-alanine (BMAA) as a widely occurring putative pathogenic factor in neurodegenerative diseases. Microorganisms 10(12): 2418. https://doi.org/10.3390/microorganisms10122418
7. de Munck E, Muñoz-Sáez E, Miguel BG, Solas MT, Ojeda I, Martínez A, Gil C, Arahuetes RM (2013) β-N-methylamino-l-alanine causes neurological and pathological phenotypes mimicking Amyotrophic Lateral Sclerosis (ALS): the first step towards an experimental model for sporadic ALS. Environ Toxicol Pharmacol. 36(2): 243-255. doi: 10.1016/j.etap.2013.04.007.

8. Patton EE, Zon LI, Langenau DM. (2021) Zebrafish disease models in drug discovery: from preclinical modelling to clinical trials. Nat Rev Drug Discov. 20(8): 611-628. doi: 10.1038/s41573-021-00210-8.
9. Fernández-Ruiz J, Sagredo O, Pazos MR, García C, Pertwee R, Mechoulam R, Martínez-Orgado J (2013). Cannabidiol for neurodegenerative disorders: important new clinical applications for this phytocannabinoid? British J Clinical Pharmacol. 75(2): 323-333. https://doi.org/10.1111/j.1365-2125.2012.04341.x
10. Aychman MM, Goldman DL, Kaplan JS. (2023) Cannabidiol's neuroprotective properties and potential treatment of traumatic brain injuries. Front Neurol. 14: 1087011. doi: 10.3389/fneur.2023.1087011.
11. Kim J, Choi P, Park YT, Kim T, Ham J, Kim JC (2023). The cannabinoids, CBDA and THCA, rescue memory deficits and reduce amyloid-beta and tau pathology in an Alzheimer's disease-like mouse model. Int J Molec Sci. 24(7): 6827. https://doi.org/10.3390/ijms24076827
12. Del Prado-Audelo ML, Cortés H, Caballero-Florán IH, González-Torres M, Escutia-Guadarrama L, Bernal-Chávez SA, Giraldo-Gomez DM, Magaña JJ, Leyva-Gómez G (2021). Therapeutic applications of terpenes on inflammatory diseases. Front Pharmacol. 12: 704197. https://doi.org/10.3389/fphar.2021.704197
13. André R, Gomes AP, Pereira-Leite C, Marques-da-Costa A, Monteiro Rodrigues L, Sassano M, Rijo P, Costa MDC (2024). The entourage effect in cannabis medicinal products: a comprehensive review. Pharmaceuticals (Basel, Switzerland) 17(11): 1543. https://doi.org/10.3390/ph17111543
14. Russo EB (2011). Taming THC: potential cannabis synergy and phytocannabinoid-terpenoid entourage effects. Br J Pharmacol 163(7): 1344-1364. https://doi.org/10.1111/j.1476-5381.2011.01238.x
15. Erridge S, Mangal N, Salazar O, Pacchetti B, Sodergren MH (2020). Cannflavins - From plant to patient: A scoping review. Fitoterapia 146: 104712. doi:10.1016/j.fitote.2020.104712
16. Barrett ML, Gordon D, Evans FJ (1985). Isolation from cannabis sativa L. of cannflavin - a novel inhibitor of prostaglandin production. Biochem Pharmacol 34(11): 2019-2024. https://doi.org/10.1016/0006-2952(85)90325-9
17. Krokidis MG, Vlamos P (2018) Transcriptomics in amyotrophic lateral sclerosis. Front Biosci (Elite Ed). 10(1): 103-121. doi: 10.2741/e811.
18. Rizzuti M, Sali L, Melzi V, Scarcella S, Costamagna G, Ottoboni L, Quetti L, Brambilla L, Papadimitriou D, Verde F, Ratti A, Ticozzi N, Comi GP, Corti S, Gagliardi D (2023) Genomic and transcriptomic advances in amyotrophic lateral sclerosis. Ageing Res Rev. 92: 102126. doi: 10.1016/j.arr.2023.102126.
19. Lissouba A, Liao M, Kabashi E, Drapeau P (2018) Transcriptomic Analysis of Zebrafish TDP-43 Transgenic Lines. Front Mol Neurosci. 11: 463. doi: 10.3389/fnmol.2018.00463
20. Bilsland LG, Dick JR, Pryce G, Petrosino S, Di Marzo V, Baker D, Greensmith L (2006) Increasing cannabinoid levels by pharmacological and genetic manipulation delay disease progression in SOD1 mice. FASEB J. 20(7): 1003-1005. doi: 10.1096/fj.05-4743fje
21. Shoemaker JL, Seely KA, Reed RL, Crow JP, Prather PL (2007) The CB2 cannabinoid agonist AM-1241 prolongs survival in a transgenic mouse model of amyotrophic lateral sclerosis when initiated at symptom onset. J Neurochem. 101(1): 87-98. doi: 10.1111/j.1471-4159.2006.04346.x.

22. Luchtenburg FJ, Schaaf MJM, Richardson MK (2019). Functional characterization of the cannabinoid receptors 1 and 2 in zebrafish larvae using behavioral analysis. Psychopharmacol 236(7): 2049-2058. https://doi.org/10.1007/s00213-019-05193-4
23. Martin M (2011). Cutadapt removes adapter sequences from high-throughput sequencing reads. EMBnet J 17(1): 10–12.
24. Dobin A, Davis CA, Schlesinger F, Drenkow J, Zaleski C, Jha S, Batut P, Chaisson M, Gingeras TR (2013). STAR: ultrafast universal RNA-seq aligner. Bioinformatics 29(1): 15–21. https://doi.org/10.1093/bioinformatics/bts635
25. Dobin A, Gingeras TR (2015). Mapping RNA-seq reads with STAR. Current Protocols in Bioinformatics 51: 11.14.1-11.14.19. https://doi.org/10.1002/0471250953.bi1114s51
26. Andrews S (2010). FastQC: a quality control tool for high throughput sequence data. In Babraham.ac.uk. https://www.bioinformatics.babraham.ac.uk/projects/fastqc/
27. Love MI, Huber W, Anders S (2014). Moderated estimation of fold change and dispersion for RNA-seq data with DESeq2. Genome Biol 15: 550. https://doi.org/10.1186/s13059-014-0550-8
28. Banwait I, Deol G (2025). DEG Pipeline Assistant: An interactive and reproducible pipeline for rna-seq differential expression and pathway analysis. ResearchHub (preprint) https://www.researchhub.com/paper/9398712/deg-pipeline-assistant-an-interactive-and-reproducible-pipeline-for-rna-seq-differential-expression-and-pathway-analysis
29. Son K, Yu S, Shin W, Han K, Kang K (2018). A Simple Guideline to Assess the Characteristics of RNA-Seq Data. BioMed Res Int 2018:2906292. https://doi.org/10.1155/2018/2906292
30. Rowland A, Miners JO, Mackenzie PI (2013). The UDP-glucuronosyltransferases: Their role in drug metabolism and detoxification. Int J Biochem Cell Biol 45(6): 1121–1132. https://doi.org/10.1016/j.biocel.2013.02.019
31. Liu Y, Xi Y, Chen G, Wu X, He M (2020). URG4 mediates cell proliferation and cell cycle in osteosarcoma via GSK3β/β-catenin/cyclin D1 signaling pathway. J Orthop Surg Res 15(1): 226. https://doi.org/10.1186/s13018-020-01681-y
32. Singh D (2022). Astrocytic and microglial cells as the modulators of neuroinflammation in Alzheimer's disease. J Neuroinflam 19(1): 206. https://doi.org/https://doi.org/10.1186/s12974-022-02565-0
33. Li K, Chen Z, Chang X, Xue R, Wang H, Guo W (2024). Wnt signaling pathway in spinal cord injury: from mechanisms to potential applications. Front Mol Neurosci 17: 1427054. https://doi.org/10.3389/fnmol.2024.1427054
34. Sasabe J, Miyoshi Y, Suzuki M, Mita M, Konno R, Matsuoka M, Hamase K, Aiso S (2011). D-Amino acid oxidase controls motoneuron degeneration through D-serine. Proc Nat Acad Sci. USA, 109(2): 627-632. https://doi.org/10.1073/pnas.1114639109
35. Kondori NR, Paul P, Robbins JP, Liu K, Hildyard JCW, Wells DJ, de Belleroche JS (2018) Focus on the role of d-serine and d-amino acid oxidase in amyotrophic lateral sclerosis/motor neuron disease (ALS). Front Mol Biosci. 5: 8. doi: 10.3389/fmolb.2018.00008.
36. Youn Lee J, Young Choi H, Ahn H-J, Gun Ju B, Young Yune T (2014). Matrix Metalloproteinase-3 Promotes Early Blood–Spinal Cord Barrier Disruption and Hemorrhage and Impairs Long-Term Neurological Recovery after Spinal Cord Injury. Am J Pathol, 184(11): 2985–3000. https://doi.org/10.1016/j.ajpath.2014.07.016

37. Poveda J, Sanz AB, Fernandez-Fernandez B, Carrasco S, Ruiz-Ortega M, Cannata-Ortiz P, Ortiz A, Sanchez-Niño MD (2017). MXRA5 is a TGF-β1-regulated human protein with anti-inflammatory and anti-fibrotic properties. J Cell Mol Med, 21(1): 154–164. https://doi.org/10.1111/jcmm.12953
38. MedlinePlus Genetics. (2023). HLA-DQA1 gene. U.S. National Library of Medicine. https://medlineplus.gov/genetics/gene/hla-dqa1/
39. Rudy GB, Lew AM (1997). The nonpolymorphic MHC class II isotype, HLA-DQA2, is expressed on the surface of B lymphoblastoid cells. J Immunol 158(5): 2116–2125. https://doi.org/10.4049/jimmunol.158.5.2116
40. Neumann H, Misgeld T, Matsumuro K, Wekerle H (1998). Neurotrophins inhibit major histocompatibility class II inducibility of microglia: Involvement of the p75 neurotrophin receptor. Proc Nat Acad Sci. USA 95(10): 5779–5784. https://doi.org/10.1073/pnas.95.10.5779
41. Schormann N, Ricciardi R, Chattopadhyay D (2014). Uracil-DNA glycosylases-Structural and functional perspectives on an essential family of DNA repair enzymes. Protein Sci 23(12): 1667–1685. https://doi.org/10.1002/pro.2554
42. Chiu AS, Gehringer MM, Braidy N, Guillemin GJ, Welch JH, Neilan BA (2012). Excitotoxic potential of the cyanotoxin β-methyl-amino-l-alanine (BMAA) in primary human neurons. Toxicon, 60(6): 1159–1165. https://doi.org/10.1016/j.toxicon.2012.07.169
43. Kok JR, Palminha NM, Dos Santos Souza C, El-Khamisy SF, Ferraiuolo L (2021). DNA damage as a mechanism of neurodegeneration in ALS and a contributor to astrocyte toxicity. Cell Mol Life Sci 78(15): 5707–5729. https://doi.org/10.1007/s00018-021-03872-0
44. Ghorbani S, Yong VW (2021). The extracellular matrix as modifier of neuroinflammation and remyelination in multiple sclerosis. Brain 144(7): 1958–1973. https://doi.org/10.1093/brain/awab059
45. Maguire G (2017). Amyotrophic lateral sclerosis as a protein level, non-genomic disease: Therapy with S2RM exosome released molecules. World J Stem Cells 9(11): 187–202. https://doi.org/10.4252/wjsc.v9.i11.187
46. Komine O, Yamanaka K (2015). Neuroinflammation in motor neuron disease. Nagoya J Med Sci 77(4): 537–549. https://pmc.ncbi.nlm.nih.gov/articles/PMC4664586/#sec13
47. Liu Jia, Wang F (2017). Role of neuroinflammation in amyotrophic lateral sclerosis: cellular mechanisms and therapeutic implications. Front Immunol 8: 1005. https://doi.org/10.3389/fimmu.2017.01005
48. Leal SS, Gomes CM (2015). Calcium dysregulation links ALS defective proteins and motor neuron selective vulnerability. Front Cell Neurosci 9: 225. https://doi.org/10.3389/fncel.2015.00225
49. Grosskreutz J, Van Den Bosch L, Keller BU (2010). Calcium dysregulation in amyotrophic lateral sclerosis. Cell Calcium 47(2): 165–174. https://doi.org/10.1016/j.ceca.2009.12.002
50. Guatteo E, Carunchio I, Pieri M, Albo F, Canu N, Mercuri NB, Zona C (2007). Altered calcium homeostasis in motor neurons following AMPA receptor but not voltage-dependent calcium channels' activation in a genetic model of amyotrophic lateral sclerosis. Neurobiol Dis 28(1): 90–100. https://doi.org/10.1016/j.nbd.2007.07.002
51. Garcia-Segura LM, Balthazart J (2009). Steroids and neuroprotection: New advances. Front Neuroendocrinol 30(2): 5–9. https://doi.org/https://doi.org/10.1016/j.yfrne.2009.04.006

52. Borowicz KK, Piskorska B, Banach M, Czuczwar SJ (2011). Neuroprotective actions of neurosteroids. Front Endocrinol 2:50. https://doi.org/10.3389/fendo.2011.00050
53. Puig-Bosch X, Ballmann M, Bieletzki S, Antkowiak B, Rudolph U, Zeilhofer HU, Rammes G (2023). Neurosteroids mediate neuroprotection in an in vitro model of hypoxic/hypoglycaemic excitotoxicity via δ-GABAA receptors without affecting synaptic plasticity. Int J Mol Sci 24(10): 9056. https://doi.org/10.3390/ijms24109056
54. Brann D W, Dhandapani K, Wakade C, Mahesh VB, Khan MM (2007). Neurotrophic and neuroprotective actions of estrogen: Basic mechanisms and clinical implications. Steroids, 72(5): 381–405. https://doi.org/10.1016/j.steroids.2007.02.003
55. Bustamante-Barrientos FA, Méndez-Ruette M, Ortloff A, Luz-Crawford P, Rivera FJ, Figueroa CD, Molina L, Bátiz LF (2021). The impact of estrogen and estrogen-like molecules in neurogenesis and neurodegeneration: Beneficial or harmful? Front Cell Neurosci 15: 636176. https://doi.org/10.3389/fncel.2021.636176
56. Cardona-Rossinyol A, Mir M, Caraballo-Miralles V, Lladó J, Olmos G (2013). Neuroprotective effects of estradiol on motoneurons in a model of rat spinal cord embryonic explants. Cell Mol Neurobiol 33(3): 421–432. https://doi.org/10.1007/s10571-013-9908-9
57. Chen J, Hu R, Ge H, Duanmu W, Li Y, Xue X, Hu S, Feng H (2015). G-protein-coupled receptor 30-mediated antiapoptotic effect of estrogen on spinal motor neurons following injury and its underlying mechanisms. Mol Med Rep 12(2): 1733–1740. https://doi.org/10.3892/mmr.2015.3601
58. Munteanu C, Galaction AI, Turnea M, Blendea CD, Rotariu M, Poștaru M (2024). Redox homeostasis, gut microbiota, and epigenetics in neurodegenerative diseases: A systematic review. Antioxidants, 13(9): 1062. https://doi.org/10.3390/antiox13091062
59. Rice ME (2000). Ascorbate regulation and its neuroprotective role in the brain. Trends Neurosci 23(5), 209-216. https://doi.org/10.1016/s0166-2236(99)01543-x
60. Plascencia-Villa G, Perry G (2023). Roles of oxidative stress in synaptic dysfunction and neuronal cell death in Alzheimer's disease. Antioxidants 12(8): 1628. https://doi.org/10.3390/antiox12081628
61. Petrovic S, Arsic A, Ristic-Medic D, Cvetkovic Z, Vucic V (2020). Lipid peroxidation and antioxidant supplementation in neurodegenerative diseases: A review of human studies. Antioxidants 9(11): 1128. https://doi.org/10.3390/antiox9111128
62. Yan Y, Zhang A, Dong H, Ge Y, Sun H, Wu X, Han Y, Wang X (2017). Toxicity and detoxification effects of herbal Caowu via ultra performance liquid chromatography/mass spectrometry metabolomics analyzed using pattern recognition method. Pharmacogn Mag 13(52): 683–692. https://doi.org/10.4103/pm.pm_475_16
63. Sun H, Zhang A, Song Q, Fang H, Liu X, Su J, Yang L, Yu M, Wang X (2018). Functional metabolomics discover pentose and glucuronate interconversion pathways as promising targets for Yang Huang syndrome treatment with Yinchenhao Tang. RSC Advances 8(64): 36831-36839. https://doi.org/10.1039/c8ra06553e
64. Snyder MJ (2000). Cytochrome P450 enzymes in aquatic invertebrates: recent advances and future directions. Aquatic Toxicol 48(4): 529–547. https://doi.org/10.1016/s0166-445x(00)00085-0

65. Liu J, Zhang D, Zhang L, Wang Z, Shen J (2022). New insight on vitality differences for the Penaeid shrimp, *Fenneropenaeus chinensis*, in low salinity environment through transcriptomics. Front Ecol Evol 10: 716018. https://doi.org/10.3389/fevo.2022.716018
66. Rai SN, Dilnashin H, Birla H, Singh SS, Zahra W, Rathore AS, Singh BK, Singh SP (2019). The role of PI3K/Akt and ERK in neurodegenerative disorders. Neurotox Res 35: 775–795. https://doi.org/10.1007/s12640-019-0003-y
67. Chen Y, Hsu C, Chen X, Zhang H, Peng W (2023). Editorial: Regulation of PI3K/Akt signaling pathway: A feasible approach for natural neuroprotective agents to treat various neuron injury-related diseases. Front Pharmacol 14: 1134989. https://doi.org/10.3389/fphar.2023.1134989
68. Qi Y, Yang C, Zhao H, Deng Z, Xu J, Liang W, Sun Z, Dirk J (2022). Neuroprotective effect of sonic hedgehog mediated PI3K/AKT pathway in amyotrophic lateral sclerosis model mice. Molec Neurobiol 59: 6971–6982. https://doi.org/10.1007/s12035-022-03013-z
69. Singh P, Belliveau P, Towle J, Neculau AE, Dima L (2024). Edaravone oral suspension: A neuroprotective agent to treat amyotrophic lateral sclerosis. Am J Ther 31(3): 258–267. https://doi.org/10.1097/MJT.0000000000001742
70. Stielow M, Witczyńska A, Kubryń N, Fijałkowski Ł, Nowaczyk J, Nowaczyk A (2023). The bioavailability of drugs – The current state of knowledge. Molecules 28(24): 8038. https://doi.org/10.3390/molecules28248038

ACKNOWLEDGEMENTS

The authors thank Ethan Russo, MD, for his advice in interpreting the results, and Helia Ghazinejad, MBI, for assistance with preliminary data analysis. BMAA-treatment model, product efficacy assessment, and phenotypic analysis were developed and performed by CREM Co Labs (Mississauga, Ontario).

FUNDING

RNA extraction and sequencing were funded by the NRC Industrial Research Assistance Program (NRC-IRAP). All other parts of this research were funded by Canurta Therapeutics.

AUTHOR CONTRIBUTIONS

K.B., E.S., and A.G. conceived and designed the experiments. K.B., E.S., and F.K. carried out the experiments. J.A.C. provided scientific advice throughout all steps. I.B. and G.D. analyzed the data. I.B. and J.A.C. wrote the manuscript. All authors read and approved the final manuscript.

DATA AND CODE AVAILABILITY

All data generated and analyzed during this study are provided in the Supplementary Material, which can be found at https://figshare.com/projects/Transcriptomic_Analysis_of_Neuroprotective_Therapies_in_a_Zebrafish_Model_of_ALS/251624. This includes the product toxicity assay results, original normalized RNA-seq data, and the complete set of downstream differential expression data for all 20 experimental comparisons. Additional figures such as volcano plots, MA plots, heatmaps, and enrichment barplots are also available in the Supplementary Material.

All code for the pipeline used for analysis (the DEG Pipeline Assistant) is available at https://github.com/Shaan7071/DEG-pipeline-assistant. Further information or materials can be requested from the corresponding author.

CONFLICTS OF INTEREST

This research was funded by Canurta Therapeutics, to which the authors belong.

ETHICAL APPROVAL

All experimental procedures were approved by the Zebrafish Care Committee at the Zebrafish Centre for Drug Discovery, CREM Co Labs, Mississauga, Canada (SOP #ZFG04, Rev 00) in accordance with the guidelines of the Canadian Council on Animal Care (CCAC) for zebrafish maintenance and husbandry.

CONSENT TO PARTICIPATE

Consent was not required for the performed study.